

**Utilization of Pathway Modeling to Predict Changes in  
Sphingolipid Content During Granulocytic Differentiation of  
Retinoic Acid-induced HL60 cells**

---

**Georgia Institute of Technology**

**School of Biology**

**Brent Portz**

**Faculty Advisor: Dr. Al Merrill  
Second Reader: Dr. Marion Sewer  
April 19, 2009**

**Undergraduate Honors Thesis for the Partial Fulfillment of  
Research Option within the School of Biology**

## **Abstract**

Genomic analyses have the potential to provide insight to metabolic pathways and biomolecules that are important in cellular processes. This study used a recently developed tool (GenMAPP v2.1, [www.genmapp.org](http://www.genmapp.org) adapted for the human sphingolipid biosynthesis pathway, [www.sphingomap.org](http://www.sphingomap.org)) to compare published gene expression data for HL60 cells, a human promyelocytic leukemia cell line, treated with retinoic acid to induce granulocytic differentiation. Based on the location and magnitude of changes in expression of genes for enzymes of sphingolipid metabolism in the context of this pathway model, granulocytic differentiation would be predicted to elevate *de novo* sphingolipid biosynthesis due to higher expression of serine palmitoyltransferase, with some interesting shifts in the way that the sphingoid base (sphinganine) is subsequently metabolized—such as that some may be incorporated into downstream metabolites such as ganglioside GD3. These predictions were tested and confirmed using thin layer chromatography. It is hoped this approach will help translate changes in gene expression for this pathway into a sphingolipidomic profile for the cells, and perhaps uncover interesting changes that can explain the behavior of these cells and possible therapeutic targets or biomarkers.

**Key Words:** Sphingolipidomics, Glycosphingolipids, ATRA, HL60, Granulocytic Differentiation, Microarray

**Abbreviations:**

HL60; Human Promyelocytic cell line

SMS; SM synthase

GLS; Glycosphingolipids

DES1; DHCer desaturase

MS; Mass Spectrometry

APL; Acute Myeloid Leukemia

ATRA; All-*trans*-Retinoic Acid

NSE; Non-specific esterase

MPO; Myeloperoxidase

Sa; sphinganine

So; sphingosine

EP; ethanolamine phosphate

Sa1P; sphinganine 1-phosphate

S1P; sphingosine 1-phosphate

Cer; ceramide

DHCer; dihydroceramide

SM; sphingomyelin

GalCer; galactosylceramide

GluCer; glucosylceramide

LacCer; lactosylceramide

## **Introduction**

Sphingolipids are a complex and highly diverse family of phospho- and glycolipids present in all eukaryotic cells. Research in recent decades has broadened the conventional functionality of these biomolecules as structural components of the plasma membrane to recognize them as mediators of signaling pathways responsible for cell growth and death [1-3]. Interest has also been directed toward the potential of sphingolipids to modulate the differentiation process of HL60 cells [1].

The human promyelocytic (HL60) cell line serves as a convenient model for studying cellular differentiation as many agents are known to modulate the ultimate cellular lineage of these cells. *All-trans*-retinoic acid (ATRA) and dimethylsulfoxide (DMSO) are known inducers of granulocytic differentiation of HL60 cells and have been shown to invoke changes in sphingolipid and glycosphingolipids (GSL) content during this process [4,5]. In HL60 cells, irregular metabolism of sphingolipids and GSLs inhibits the multipotent nature of these cells [6,7]. Multiple studies have shown accumulation of ceramide, a bioactive intermediate of the sphingolipid metabolism, to induce growth inhibition and prevents normal maturation [8-10]. Other ceramide derivatives, including sphingosine [11], sphingosine-1-phosphate [11], and glycosphingolipids especially the ganglioside GM3 [12], [2,13,14] have also been shown to modulate proliferation of HL60 cells. Prominently, the shedding of GM3 from myeloblasts membrane into the plasma upon ATRA-treatment is thought to initiate pathways responsible for continued proliferation and differentiation [15]. Bioactive sphingolipids and GSLs act to regulate an assortment of signaling pathways during stress stimuli from agents such as ATRA or DMSO [16,17]. Reference [18] reviews ceramide second messenger effects of protein

kinase C (PKC) family, c-jun N-terminal kinase (JNK), and protein phosphatase 1 (PP1) signaling pathways during differentiation. The structural complexity of sphingolipid species allow for the functional diversity of sphingolipids.

The combinatorial nature of the sphingolipid components, as shown in Fig. 1, is the source of the structural complexity found in these bioactive second messengers [19]. The multiple structural variants found within the 1) fatty acids of the ceramide backbone; acyl chains ranging in length from 14-32 carbon atoms, 2) sphingoid base backbone; fully saturated as in sphinganine and unsaturated as seen in sphingosine, and 3) polar head group; hydrogen atom (ceramide), phosphate (ceramide-1-phosphate), and carbohydrate groups (simple sugars as found in glucosylceramide and galactosylceramide or complex sugars formed during ganglioside biosynthesis) provide immense challenges when attempting to distinguish among similar components during sphingolipid analysis. Mass spectrometry (MS) has been the traditional method for analyzing cellular sphingolipid content in past decades [20] as it provides the necessary specificity to distinguish acyl chain lengths of sphingoid base backbones and fatty acids by mass determination. In addition, the high sensitivity of MS analysis permits detection at physiological levels [21]. Reference [22] and [23] review the ionization methods of electrospray (ESI) and MALDI that allow MS to be analyte specific as well as the different ion analyzers currently used for sphingolipid and glycosphingolipids analysis. While mass spectrometry is consistently developing in the ways existing and novel sphingolipids are identified and measured, a large fraction of the sphingolipidome remains to be analyzed in a quantitative and structurally specific manner.

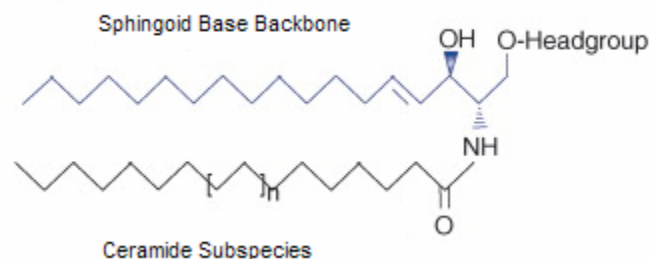


**Figure 1 - General Structure of Sphingolipid Metabolites:** Possible combinations of variations in 1) head groups 2) carbon atom lengths of ceramide subspecies and 3) saturation and carbon atom lengths of sphingoid base backbone contribute to the vast size of the sphingolipidome.

The study of sphingolipids and their related biological function is in the initial phase of shifting toward the field of systems biology as ‘omic’ studies become necessary as novel sphingolipids are determined bioactive and further expand the already immense sphingolipid profile to be examined. Such studies examine all molecular species of a given family; for sphingolipids, a true sphingolipidomic analysis would quantitatively examine all headgroups, structural variants, and combinations thereof in the metabolic pathway [24]. The quantitative abilities of MS are currently limited to a small fraction of the sphingolipidome (localized to *de novo* sphingolipids and upstream simple glycosphingolipids) due to the lack of internal standards for each analyte of sphingolipid biosynthesis; such standards control differences in conditions during ionization and sample preparation [22]. An alternative strategy when building a sphingolipidomic profile might exist in the genomic analysis of the genes responsible for catalyzing sphingolipid-associated reactions. Gene expression data may provide useful insight that relating activity levels of sphingolipid enzymes to metabolite production within the cell.

Comprehensive databases that store publicly available genomic studies, the Gene Expression Omnibus Database (GEO Database) of the NCBI for example, permit access to such gene expression data sets for analysis. On a small scale, RT-*q*PCR demonstrated a strong correlation of mRNA expression of CerS2 and production of C20-26-ceramides by LC ESI-MS/MS in Human embryonic kidney cells (Hek293) [25] suggesting gene activity can predict metabolite production. However, before confidently utilizing gene expression data to predict sphingolipid content on a larger scale, further confirmation by MS and other quantitative techniques are necessary.

Genomic analyses quickly become overwhelming as large data sets are left to be interpreted. Visualization tools permit the illustration of gene expression data in the context of pathway models and biological pathways facilitating data interpretation. KEGG pathways are commonly associated, however open source software GenMAPP v2.1 [26] and Pathvisio [27] are now available for pathway building and data visualization. Fig. 2 represents the *de novo* sphingolipid metabolism (based on the KEGG representation) created within GenMAPP. Recently, reference [28] reviewed the vast potential of these ‘omic’ tools and applicability when conducting sphingolipidomic analyses.

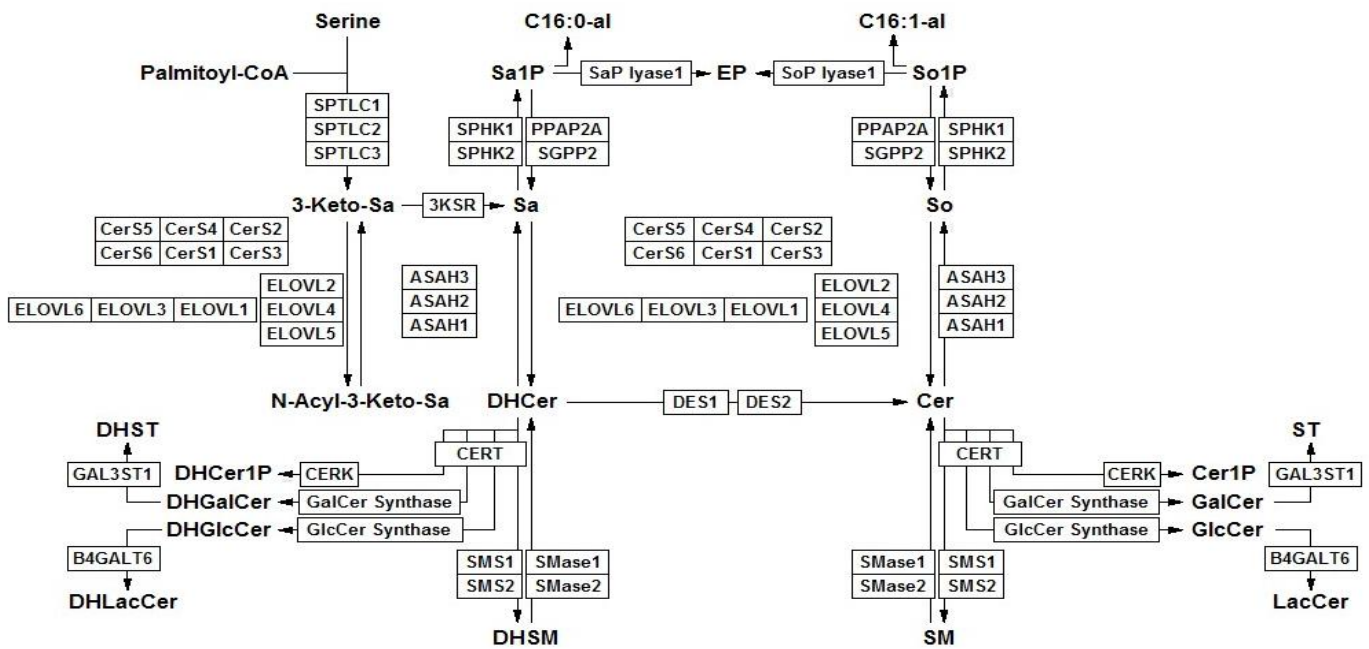


**Figure 2 - GenMAPP v2.1 representation of backbone sphingolipid biosynthesis:**

Members of this family of compounds are structurally related through a shared sphingoid base backbone (i.e. sphinganine; d18:0, sphingosine; d18:1, and others) predominantly found in mammals as 18 carbons in chain length; other structural variants and sphingoid backbones found in other organisms were recently reviewed. Subsequent *de novo* biosynthesis incorporates sphingoid bases into more complex sphingolipids. Sphinganine and sphingosine can be phosphorylated to form sphinganine 1-phosphate (Sa1P) and sphingosine 1-phosphate (So1P), respectively, or N-acylated by a family of ceramide synthases (CerS or Lass) 1-6 to synthesize (dihydro) ceramide a highly bioactive intermediate of the sphingolipid metabolism. Ceramide serves as a key precursor to additional steps of the sphingolipid biosynthesis as it is further metabolized to sphingomyelins (SM), ceramide 1-phosphate, or glycosphingolipids. Pathways illustrating further glycosphingolipid metabolism (ganglio-, globo, isoglobo-, lacto- and neolactoseries) can be found at [www.sphingomap.com](http://www.sphingomap.com).



We have taken a systems approach when analyzing the changes in sphingolipid content during the granulocytic differentiation of HL60 cells. Genomic data was viewed in the context of the sphingolipid pathways and metabolomic predictions were made based on sphingolipid enzyme activity. Interest changes were observed, possibly explaining the regulatory mechanism of sphingolipids. This technique permits the management of large data sets and ultimately allows for the prediction of changes in sphingolipid metabolites involved in granulocytic differentiation of HL60 cells. Such insight into the role of sphingolipid metabolites during this process permits subsequent investigation of these molecules as potential biomarkers and therapeutic agents used in acute myeloid leukemia (AML).

## **Methods**

### *Pathway Modeling and Microarray Analysis*

Sphingolipid pathway model as illustrated in Fig. 1 was built using open source software GenMAPP v2.1 [26] and was constructed based on the KEGG representation of the sphingolipid pathway ([www.genome.ad.jp/dbget-bin/show\\_pathway?mmu00600](http://www.genome.ad.jp/dbget-bin/show_pathway?mmu00600)). Modifications were made to include only those genes found within the mammalian genome; existing pathway included genes found within plants and yeast not relevant to this study. In addition, new isoforms of existing genes were added as well as updating preexisting gene nomenclature (i.e. LASS1-6 → CerS1-6 [29]). Pathway files for *de novo*, ganglio-, globo-, isoglobo-, lacto-, and neolactoseries can be downloaded at [www.sphingomap.com](http://www.sphingomap.com).

Microarray analysis was also conducted using GenMAPP v2.1. Gene expression data was obtained from a publicly available myeloid differentiation study [30] deposited in Gene Expression Omnibus (GEO) datasets, ID: GSE995. Expression data was mined for sphingolipid-related enzymes and imported into the pathways using enzyme Affymetrix identification numbers. Gene expression data was illustrated based on the heat scale, as shown in Fig. 3a, and was determined significant when activity was elevated >1.5 Fold or suppressed <0.67 Fold relative to the control. Instruction tutorial for pathway construction and data application is available at [www.sphingomap.com](http://www.sphingomap.com).

### *Cell Culture*

Promyeloid leukemic (HL60) cells were grown in RPMI-1640 medium (Sigma, St. Louis, MO, USA) supplemented with 10% (v/v) fetal calf serum (Invitrogen Life Technologies, Mulgrave, Victoria, Australia) and incubated at 37 °C, with 5% CO<sub>2</sub>. HL60 cells were cultured in T75 flasks and diluted to the beginning of log phase ( $2-3 \times 10^5$  cells/mL) after reaching  $1 \times 10^6$  cells/ml. Granulocytic differentiation was induced with ATRA (1  $\mu$ M) (Sigma, St. Louis, MO, USA) dissolved in 95% ethanol for a 5 day time period. Trypan blue exclusion determined cell viability and was maintained at > 95%.

### *Confirmation of Granulocytic Differentiation*

To assess morphological changes induced during granulocytic differentiation with ATRA treatment, non-specific esterase (NSE) [31] and myeloperoxidase (MPO) [32] staining were performed according to manufacture (Sigma) protocol;  $2 \times 10^6$  cells were fixed to slides for observation.

Degree of differentiation was monitored by CD11b antigen expression [33]. After ATRA time course,  $1 \times 10^6$  cells were harvested for analysis. Cells were washed twice in PBS and incubated at 4 °C in the dark for 30 minutes with mouse anti-human CD11b antibody conjugated with FITC (Sigma, St. Louis, MO, USA),  $5\mu\text{L}/1 \times 10^6$  cells [34]. Cells were further washed after incubation and suspended in 1 mL RPMI media mixture for analysis. FACS analysis was conducted using BD LSR Flow Cytometer (San Jose, California, USA).

#### *Thin Layer Chromatography*

GSL isolation was performed by Thin Layer Chromatography (TLC) as described by van Echten-Deckert, 2000 [35].  $7 \times 10^7$  cells were harvested for extraction. Method was supplemented with additional washing steps to remove polar contaminants: 8 mL chloroform/methanol (1:1,v/v), 8 mL chloroform/methanol (2:1,v/v), and 8 mL chloroform. Following purification and separation, acidic and neutral GSL extracts were dissolved in chloroform/methanol (2:1, v/v) and applied to silica-glass backed plates (Merck, Darmstadt, Germany). A solvent system of chloroform/methanol/0.22%  $\text{CaCl}_2$  (65:35:8, v/v/v) was used when running acidic GSLs to increase separation of gangliosides. GSL extracts were detected with pyrimuline reagent and captured with MultiImage Light Cabinet imager (Alpha Innotech Corporation, San Leandro, California).

## Results

### *Microarray Analysis Illustrates Changes in Gene Expression of Sphingolipid-associated Enzymes during Granulocytic Differentiation.*

Gene expression data derived from a published ATRA-treated HL60 microarray study was used to abstract sphingolipid-related genes [29]. GenMAPP v2.1 was used to import the data retrieved into the context of the sphingolipid pathways for visualization.

As shown in Fig. 3, sphingolipid metabolism was found to shift to GSL production as the activity of lactosyltransferase (B4GalT6) was found to increase 5-Fold relative to the control; lactosyltransferase catalyzes the production of lactosylceramide (LacCer), the precursor to subsequent GSL pathways. During initial ganglioside biosynthesis, GM3 is supposedly rapidly metabolized to gangliosides with multiple sialyl groups as GM3 synthase was found suppressed 0.67-fold as well as other enzymes responsible sialyl group addition are shown elevated, Fig. 3.

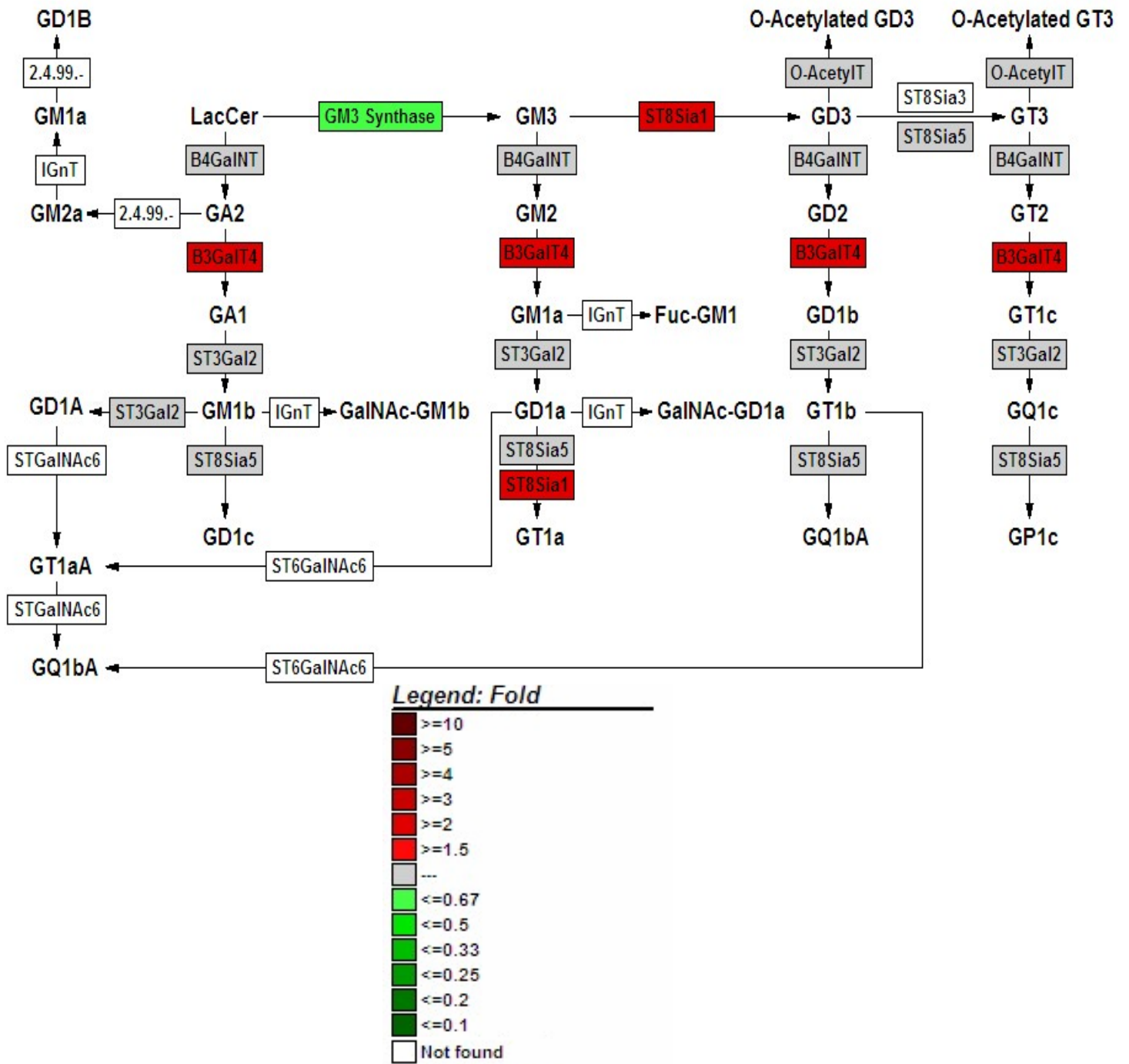


**Figure 3:** Depiction of changes in the expression of genes associated with ganglio-series sphingolipid metabolism when HL60 cells are induced to differentiate into granulocytes by retinoic acid. The gene expression data are from reference [29] and have been imported into the pathway tool and shown as the fold change in retinoic acid treated cells

versus the control. The fold change is shown by the heat scale; therefore, increases are darker red, decreases are green and gray reflects no change. Those enzymes for which data is absent are white.

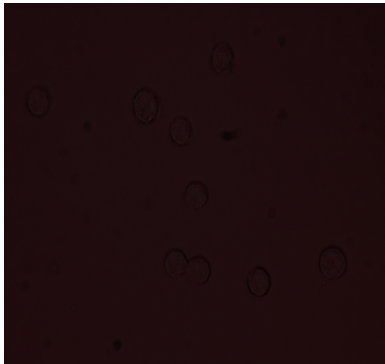
Other interesting changes in expression were found during granulocytic differentiation within the globo-, isoglobo-, lacto-, and neolactoseries during further glycosphingolipid metabolism (Supplemental 1-4).

#### *ATRA Induces Granulocytic Differentiation of HL60 cells*

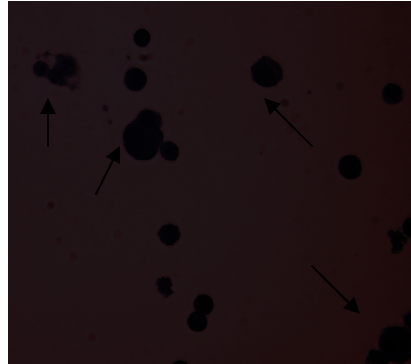
HL60 cells differentiate to neutrophil-like cells upon exposure of ATRA [4]. MPO and NSE stains were used to show characteristics of differentiated and undifferentiated HL60 cells respectively. Esterase activity was observed in the NSE stain of untreated HL60 control cells. Similarly, myeloperoxidase activity was noted in MPO stain of ATRA treated HL60 cells at both 2 and 5 day time points, while absent in undifferentiated cells, Fig. a, within Panel 1.

CD11b was used as a differentiation marker when further confirming ATRA treatment. HL60-treated cells were examined at 5 days corresponding to the treatment duration of the microarray study used in the pathway analysis [30]. Cells were also analyzed at 2 days after an independent time course study revealed 48 hr treatment to yield the highest percentage of differentiated cells, data not shown. FACS analysis reported 51% of cells to express the CD11b antigen after 2 Day ATRA (1  $\mu$ M) treatment and 60 % following 5 day ATRA treatment, Fig 4b. Both 2 and 5 day treatments were used for subsequent assays.

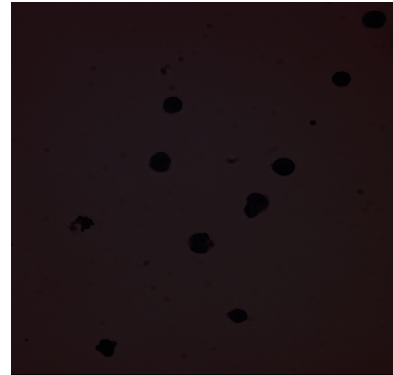
A. HL60



B. HL60 + NSE



C. ATRA + NSE

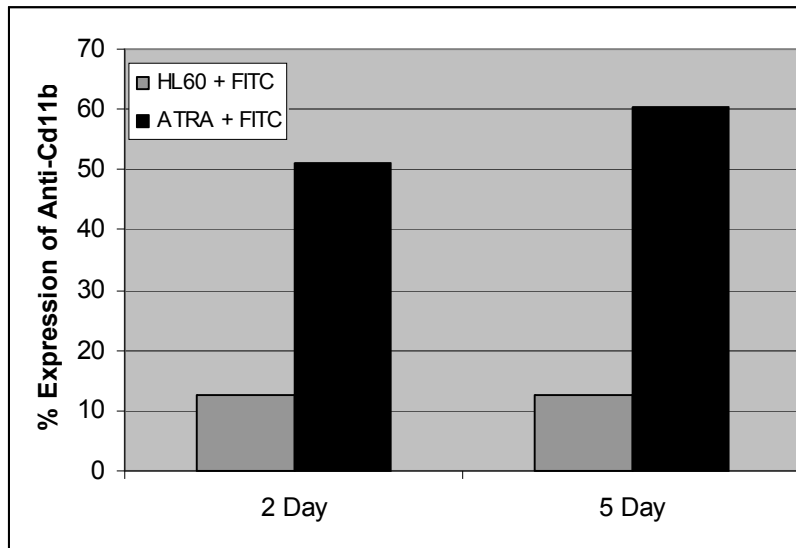


D. ATRA + MPO



E. HL60 + NSE

F.



**Panel 1 – Confirmation of ATRA-induced differentiation of HL60 cells:** NSE (non-specific esterase) stain shows undifferentiated HL60 cells as black deposits are observed during esterase activity (Fig. a,b,c); reaction strongly occurs in monocytes, while less intense in neutrophils [31]. Cells MPO (myeloperoxidase) positive for granulocytes stain brown at sites of myeloperoxidase activity (Fig. d & e); reaction is found to only take place in granulocytes and neutrophils [32]. FACS analysis, Figure f, further confirmed ATRA-induced differentiation by CD11b expression. Percentages were derived from gating the control population and subsequently measuring against the FITC tagged antibody. Results of FACS analysis are shown as one of 3 independent treatments which demonstrated similar results (2 day: 44 – 51% expression and 5 day: 52 – 60 % expression).

#### *Relationship between Sphingolipid Gene Expression and Metabolite Amounts*

Microarray analysis revealed the highest gene activity within ganglioside metabolism (Fig 3) for enzymes catalyzing the addition of sialyl groups. Therefore, we examined the monosialylated (GM1, GM2, and GM3) and disialylated (GD1, GD2, and GD3) gangliosides to assess the relationship between the changes in mRNA expression and metabolite production during granulocytic differentiation. We used TLC to (semi)-quantitatively measure the changes in GSL content.

ATRA treatment induced changes in HL60 glycosphingolipid content when analyzed by TLC (Fig. 4). While ganglioside GM3 amounts were found constant in comparison to the control after 2 days of treatment, the amounts appear to diminish by day 5. This finding was consistent with the decreased activity of GM3 synthase observed in the microarray



analysis shown in Figure 3. Similarly, a gradual increase in production of GD3 and GD1b were observed by day 5, therefore these differences in metabolite amounts are consistent with predicted gene activity levels of ST3Gal2 and B3GalT4, respectively. While GM2 production was predicted to remain constant after ATRA treatment from B4GalNT expression levels, it was found to diminish by day 5.

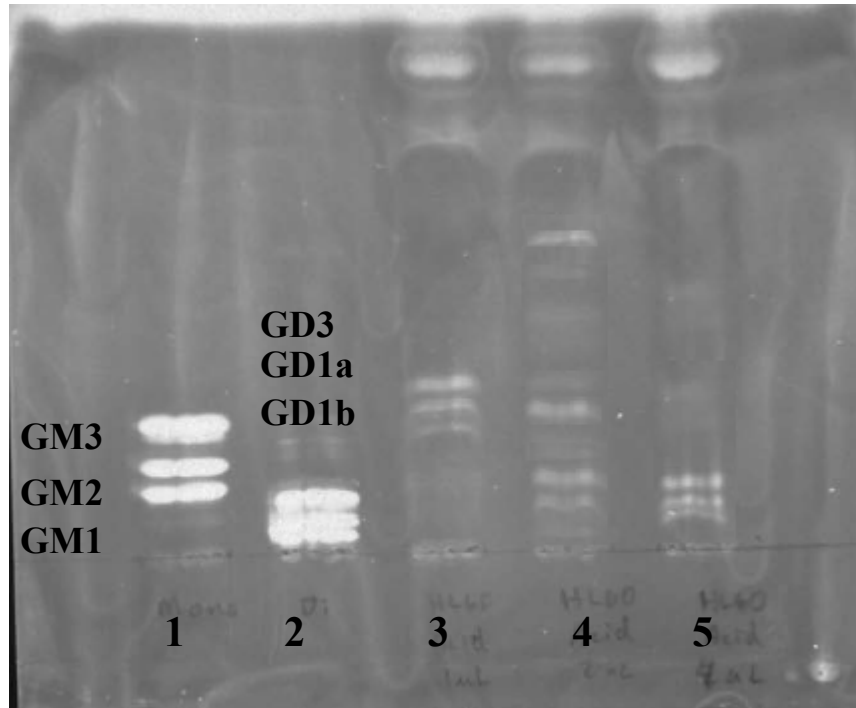


**Figure 4 – ATRA regulation of ganglioside production:** HL60 cells were treated with ATRA (1  $\mu$ M) and GSLs were collected at 2 and 5 day time periods. TLC isolated individual gangliosides using chloroform/methanol/0.22% CaCl<sub>2</sub> (65:35:8, v/v/v) and showed relative abundance during granulocytic differentiation. Lane 1 and 2 show mono- and diasialylic acid standards; from top to bottom, GM3, GM2, GM1 and GD3, GD1a, GD1b, respectively. An equal percentage (5%) of acidic GSL extract was loaded into lane 3 (undifferentiated HL60 control), lane 4 (2 day ATRA-treatment) and lane 5 (5 day

ATRA-treatment). Results shown are based on singlet analysis from 3 independent experiments.

## **Discussion**

The complex network of regulatory pathways found during granulocytic differentiation in combination with a continuously expanding profile of potential bioactive (glyco) sphingolipids requires a systems level approach when examining changes in sphingolipid content during the maturation process of HL60 cells. A systems effort when studying sphingolipids would not only examine all components of the sphingolipidome, but also determine all interactions and relationships between sphingolipid species during HL60 differentiation [36]. Sphingolipidomic tools are now necessary when comprehensively examining the sphingolipidome [24]. In the present study, we used genomic data in the context of sphingolipid and GSL biosynthetic pathways to 1) quantitatively measure a larger fraction of the sphingolipidome than traditional MS methods and 2) organize resulting data for analysis. TLC analysis, Fig. 4, confirmed genomic data predictions, Fig. 2, suggesting a correlation between mRNA expression and metabolite production within HL60 cells; summary of gene expression and metabolite production correlation discovered is shown in Table 1. Confirmation allows further predictions within the sphingolipidome until metabolite data is available.

| Ganglioside Metabolite | Gene Activity          | Predicted Metabolite Level | Observed Metabolite Level |
|------------------------|------------------------|----------------------------|---------------------------|
| GM3                    | Decreased GM3 Synthase | Decrease                   | Decrease                  |
| GM2                    | No Change B4GalNT      | No Change                  | Decrease                  |
| GM1                    | Increase B3GalT4       | Increase                   | No Change                 |
| GD1a                   | No Change ST3Gal2      | No Change                  | Increase                  |
| GD1b                   | Increase B3GalT4       | Increase                   | Increase                  |
| GD3                    | Increase ST8Sia1       | Increase                   | Increase                  |

**Table 1** – Relationship between mRNA expression and metabolite production within HL60 cells.

Based on the location and magnitude of changes in expression of genes for enzymes of sphingolipid metabolism in the context of this pathway model (Supplemental 1), granulocytic differentiation would be predicted to elevate *de novo* sphingolipid biosynthesis due to higher expression of serine palmitoyltransferase (SPTLC), but possibly with shunting of more of the intermediate sphinganine (Sa) to degradation products (hexadecanal, C16:0-al, and ethanolamine phosphate, EP) via sphinganine 1-phosphate (Sa1P). N-acylation of Sa to dihydroceramide (DHCer) is not predicted to change, except perhaps by a decrease in the proportion of subspecies with C24:0 and C24:1 fatty acids (due to lower CerS2), and more rapid conversion of DHCer to Cer by DHCer desaturase (DES1). Furthermore, DHCer and Cer are predicted to be more rapidly metabolized to sphingomyelins (SM), galactosylceramide (GalCer) and glucosylceramide (GluCer) (and downstream metabolites such as lactosylceramide, LacCer, and more complex neutral and sialyl-glycosphingolipids, Fig. 3, such as ganglioside GD3) due to elevations in the respective genes (e.g., SM synthase, SMS2, GalCer synthase, etc.), but possibly also turned over to Sa and sphingosine (So), sphingosine 1-phosphate (S1P), etc. due to elevated acid ceramidase (ASAH1). These backbone sphingolipid predictions will be tested in the future using tandem mass

spectrometry with selection of the mode of ionization (e.g., electrospray versus MALDI) and ion analyzer (e.g., quadrupole, ion trap, or time-of-flight) based on the category of analyte being examined.

It is hoped this approach will help translate changes in gene expression for this pathway into a structurally specific and quantitative sphingolipidomic profile for the cells, and perhaps uncover interesting changes further explaining the behavior of these cells and discovery of possible therapeutic targets or biomarkers used in acute myeloid leukemia (AML).

### **Acknowledgements**

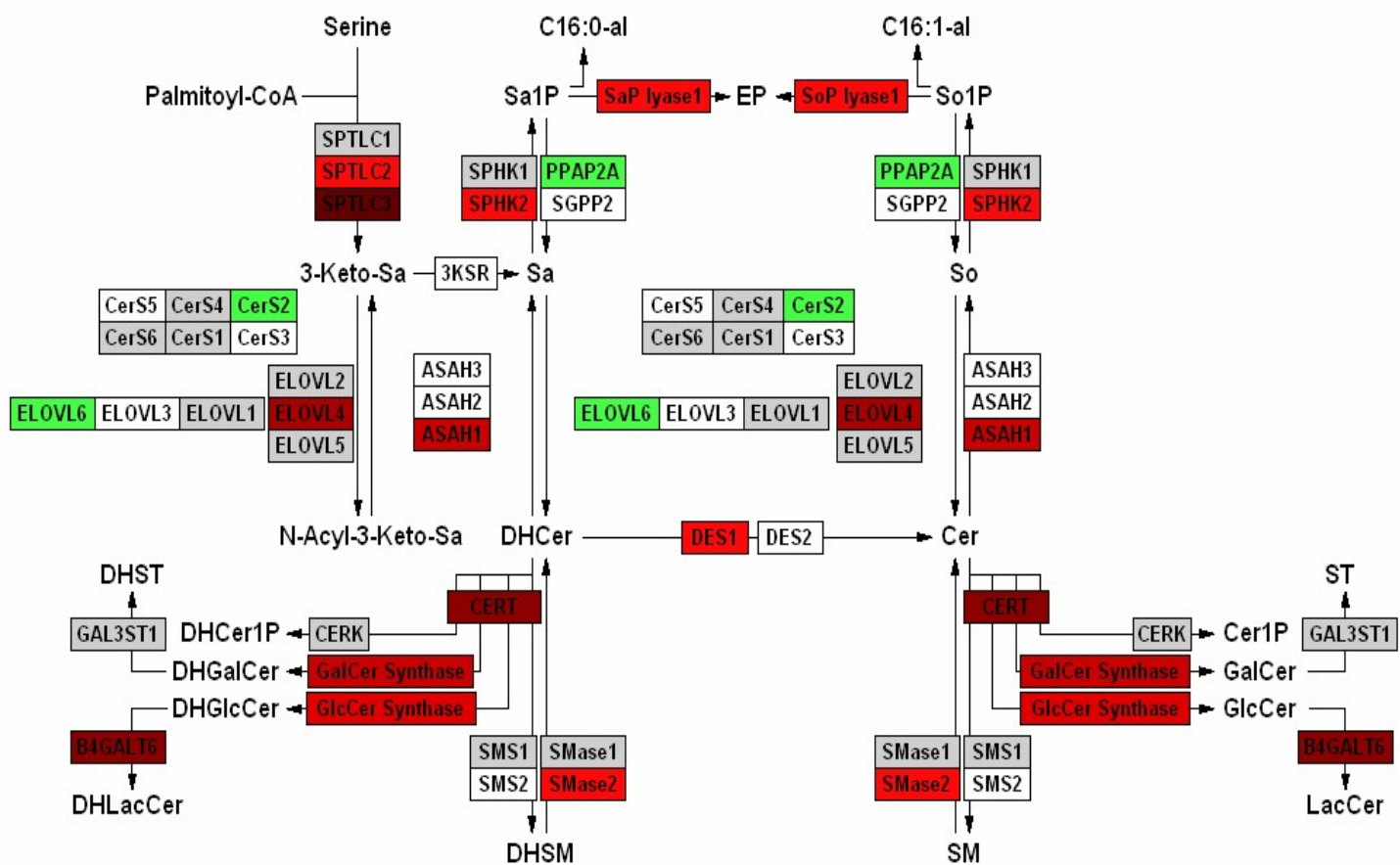
I would like to thank Dr. Merrill and group members for the time and advice given over the duration of the project. Collectively, the Merrill Lab for sparking my interest in laboratory work and a greater appreciation for science in general. Also, Elaine Wang for continuously reminding me that glycolipid extractions are “not that bad!” Furthermore, I would like to thank Dr. Sewer for advice with the writing of this manuscript. This work was supported by the Lipid MAPS Consortium grant (GM069338) (A.H.M.) and in part by funds from Microsoft Research, the National Institutes of Health (Bioengineering Research Partnership R01CA108468, P20GM072069, the Center for Cancer Nanotechnology Excellence U54CA119338), and the Georgia Cancer Coalition (M.D.W.).

## References

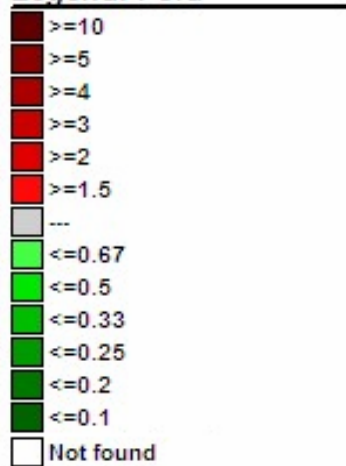
1. Spiegel S, Milstien S. Sphingoid bases and phospholipase D activation. *J. Membr. Biol.* 1995; 146: 225–37.
2. T Yamashita, R Wada, T Sasaki, C Deng, U Bierfreund, K Sandhoff and R.L Proia, A vital role for glycosphingolipid synthesis during development and differentiation, *Proc. Natl. Acad. Sci.* 1999; 96: 9142–47.
3. S Hakomori, Cell adhesion/recognition and signal transduction through glycosphingolipid microdomain, *Glycoconjugate J.* 2000; 17: 143–151.
4. TR Breitman, S.E. Selonick and S.J Collins. Induction of differentiation of the human promyelocytic leukemia cell line (HL60) by retinoic acid. *Proc Natl Acad Sci USA* 77 (1980) 2936-2940.
5. Collins SJ, Ruscetti FW, Gallagher RE, Gallo RC. Normal functional characteristics of cultured human promyelocytic leukemia cells (HL60) after induction of differentiation by dimethylsulfoxide. *J Exp Med* 149:969, 1979.
6. Alessenko AV. The role of sphingomyelin cycle metabolites in transduction of signals of cell proliferation, differentiation and death. *Membr Cell Biol.* 2000;13(2):303-20.
7. Nagatsuka Y, Hara-Yokoyama M, Kasama T, Takekoshi M, Maeda F, Ihara S, Fujiwara S, Ohshima E, Ishii K, Kobayashi T, Shimizu K, Hirabayashi Y. Carbohydrate-dependent signaling from the phosphatidylglucoside-based microdomain induces granulocytic differentiation of HL60 cells. *Proc Natl Acad Sci U S A.* 2003; 100(13):7454-9.
8. Kuo ML, Chen CW, Jee SH, Chuang SE, Cheng AL. Transforming growth factor beta1 attenuates ceramide-induced CPP32/Yama activation and apoptosis in human leukaemic HL-60 cells. *Biochem J.* 1997; 327 (Pt 3):663-7.
9. Kondo T, Matsuda T, Tashima M, Umehara H, Domae N, Yokoyama K, Uchiyama T, Okazaki T. Suppression of heat shock protein-70 by ceramide in heat shock-induced HL-60 cell apoptosis. *J Biol Chem.* 2000; 275(12):8872-9.
10. N.S Radin, Killing cancer cells by poly-drug elevation of ceramide levels. A hypothesis whose time is come?, *Eur. J. Biochem.* 2001; 268: 193–204.
11. Kee TH, Vit P, Melendez AJ. Sphingosine kinase signalling in immune cells. *Clin Exp Pharmacol Physiol.* 2005;32(3):153-61.

12. D Kalka, C Reitzenstein, J Kopitz and M Cantz, The plasma membrane ganglioside sialidase cofractionates with markers of lipid rafts, *Biochem. Biophys. Res. Commun.* 2001;283: 989–93.
13. T Arai, A.K Bhunia, S Chatterjee and G.B Bulkley, Lactosylceramide stimulates human neutrophils to upregulate Mac-1, adhere to endothelium, and generate reactive oxygen metabolites in vitro, *Circ. Res.* 1998; 82: 540–47.
14. S Hakomori, Structure, organization and function of glycosphingolipids in membrane, *Curr. Opin. Hematol.* 2003;10; 16–24.
15. Smoleńska-Sym G, Spychalska J, Zdebska E, Woźniak J, Traczyk Z, Pszenna E, Maj S, Danikiewicz W, Bieńkowski T, Kościelak J. Ceramides and glycosphingolipids in maturation process: leukemic cells as an experimental model. *Blood Cells Mol Dis.* 2004; 33(1): 68-76.
16. Hannun YA, Luberto C. Ceramide in the eukaryotic stress response. *Trends Cell Biol* 2000; 10: 73-80.
17. Jarvis WD, Fornari FA, Browning JL, Gewirtz DA, Kolesnick RN, Grant S. Attenuation of ceramide-induced apoptosis by diglyceride in human myeloid leukemia cells. *J Biol Chem* 1994; 269: 31685-31692.
18. Ruvolo PP. Ceramide regulates cellular homeostasis via diverse stress signaling pathways. *Leukemia* 2001; 15(8): 1153-1160.
19. Kolter T, Proia RL, Sandhoff K. Combinatorial Ganglioside Biosynthesis. *J. Biol. Chem.* 277 (2002), pp. 25859–62.
20. Samuelsson B, Samuelsson L. Separation and identification of ceramides derived from human plasma sphingomyelins. *J Lipid Res.* 1969 Jan;10(1):47-55.
21. Ballou LR, Laulederkind SJ, Rosloniec EF, Raghov R. Ceramide signalling and the immune response. *Biochim Biophys Acta.* 1996; 1301(3):273-87.
22. Merrill AH Jr, Sullards MC, Allegood JC, Kelly S, Wang E. Sphingolipidomics: high-throughput, structure-specific, and quantitative analysis of sphingolipids by liquid chromatography tandem mass spectrometry. *Methods.* 2005 Jun;36(2):207-24.
23. Sullards MC, Allegood JC, Kelly S, Wang E, Haynes CA, Park H, Chen Y, Merrill AH Jr. Structure-specific, quantitative methods for analysis of sphingolipids by liquid chromatography-tandem mass spectrometry: "inside-out" sphingolipidomics. *Methods Enzymol.* 2007;432:83-115.

24. Merrill, AH. Jr., Wang, MD, Park M, Sullards MC. (Glyco)sphingolipidology: an amazing challenge and opportunity for systems biology. *Trends Biochemical Science* (2007) 32:10; 457-68.
25. Laviad EL, Albee L, Pankova-Kholmyansky I, Epstein S, Park H, Merrill AH Jr, Futerman AH. Characterization of ceramide synthase 2: tissue distribution, substrate specificity, and inhibition by sphingosine 1-phosphate. *J Biol Chem.* 2008; 283(9):5677-84.
26. Dahlquist, KD, Salomonis N, Vranizan K, Lawlor SC, and Conklin BR. GenMAPP, a new tool for viewing and analyzing microarray data on biological pathways. *Nat. Genet.* 2002; 31: 19–20.
27. van Iersel MP, Kelder T, Pico AR, Hanspers K, Coort S, Conklin BR, Evelo C. Presenting and exploring biological pathways with PathVisio. *BMC Bioinformatics.* 2008 Sep 25;9:399.
28. Merrill, AH Jr., Stokes TH, Momin A, Park H, Portz BJ, Kelly S, Wang E, Sullards MC, and Wang MD. Sphingolipidomics: a valuable tool for understanding the roles of sphingolipids in biology and disease. *J. Lipid Res.* 2009. 50: S97–S102.
30. Stegmaier K, Ross KN, Colavito SA, O'Malley S, Stockwell BR, Golub TR. Gene expression-based high-throughput screening (GE-HTS) and application to leukemia differentiation. *Nat Genet.* 2004; 36(3):257-63.
31. Okazaki T, Mochizuki T, Tashima M, Sawada H, Uchino H. Magnesium deprivation inhibits the expression of differentiation-related phenotypes in human promyelocytic leukemia HL-60 cells. *J Cell Physiol.* 1987; 131(1):50-7.
32. Graham RC, Karnovsky MJ: Glomerular permeability. Ultrastructural cytochemical studies using peroxidases as protein tracers. *J Exp Med.* 1966; 124:1123
33. Tomonaga M, Golde D, Gasson J. Biosynthetic (recombinant) human granulocyte-macrophage colony-stimulating factor: effect on normal bone marrow and leukemia cell lines. *Blood.* 1986; 67:31-36.
34. Barkley LR, Hong HK, Kingsbury SR, James M, Stoeber K, Williams GH. Cdc6 is a rate-limiting factor for proliferative capacity during HL60 cell differentiation. *Exp Cell Res.* 2007; 313(17):3789-99.
35. van Echten-Deckert G. Sphingolipid extraction and analysis by thin-layer chromatography. *Methods Enzymol.* 2000; 312:64-79.
36. Aderem A. Systems biology: its practice and challenges, *Cell.* 2005; 121, pp. 511–513.

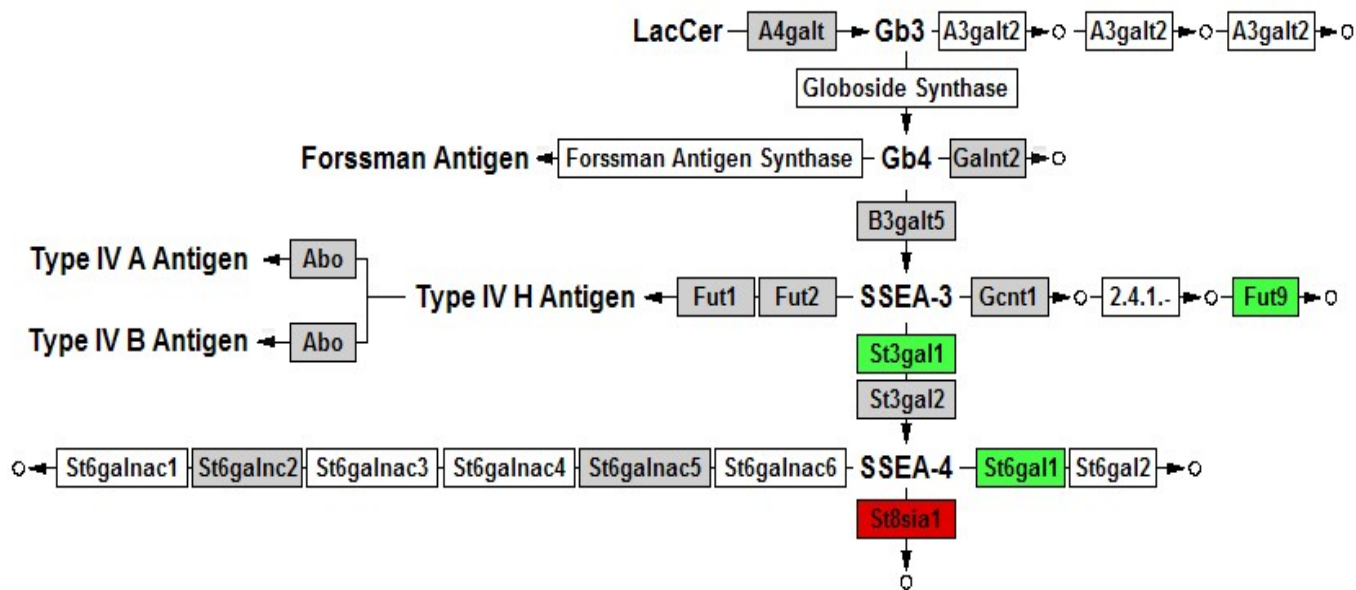


**Legend: Fold**

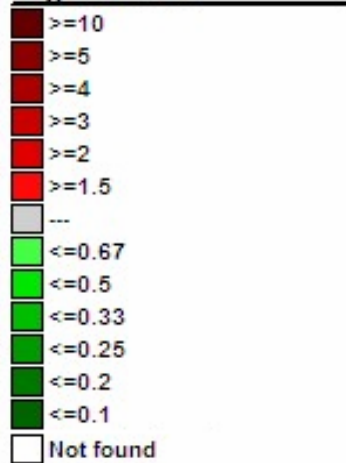


**Supplemental Figure 1: Backbone Sphingolipid Biosynthesis**

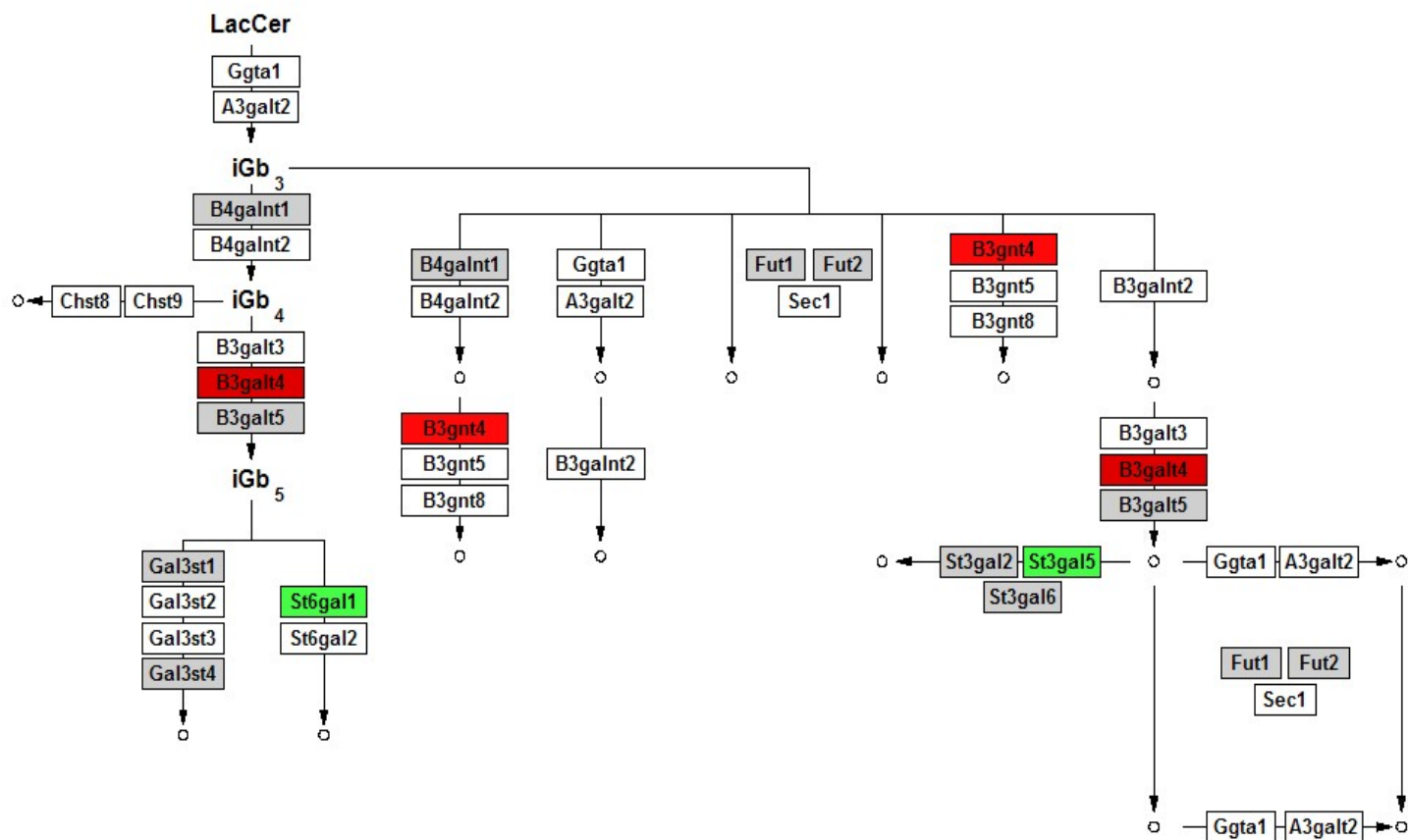




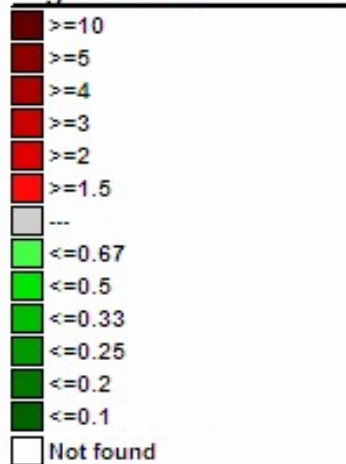
**Legend: Fold**



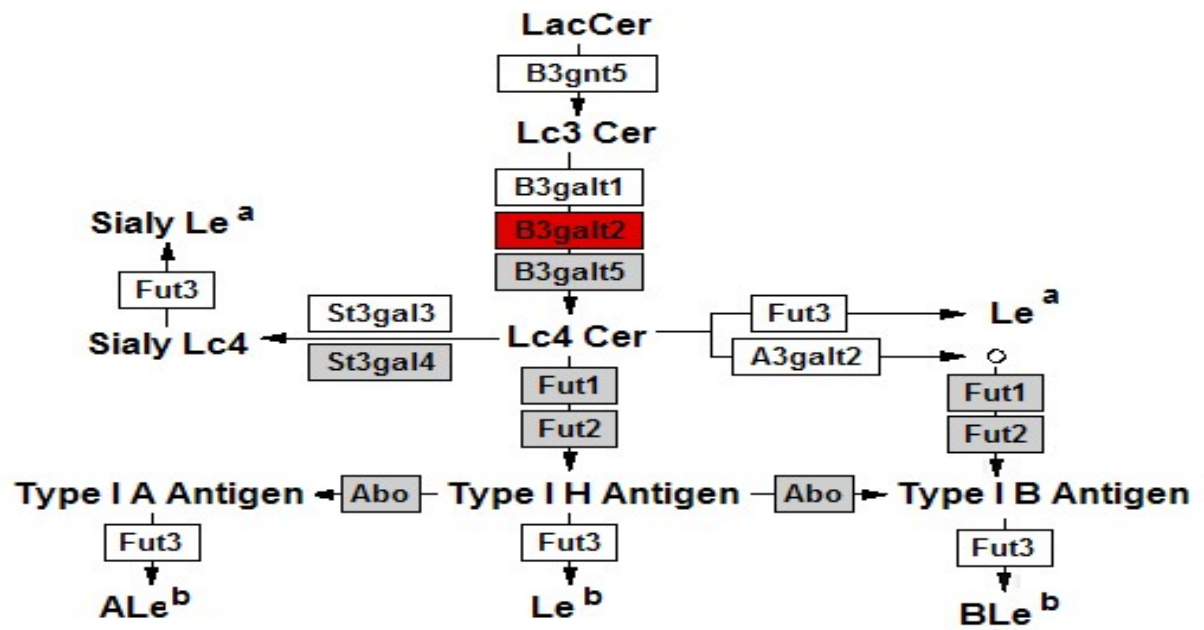
**Supplemental Figure 2: Globoseries Biosynthesis**



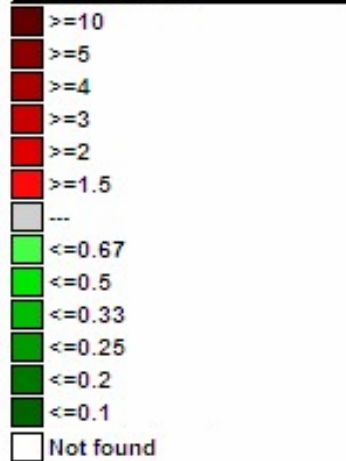
**Legend: Fold**



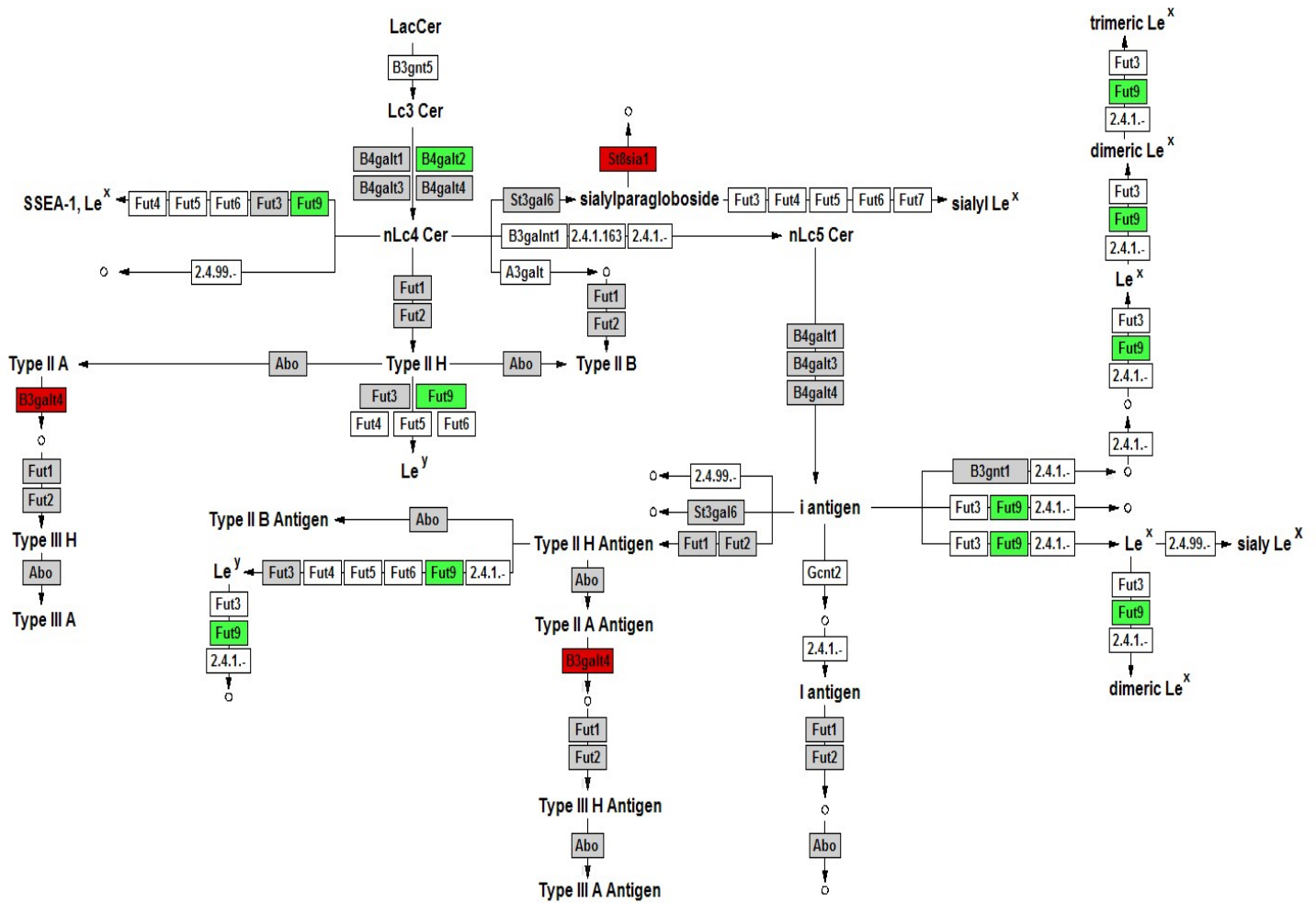
**Supplemental Figure 3: Isogloboseries Biosynthesis**



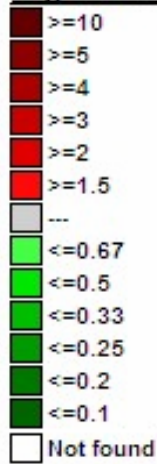
*Legend: Fold*



Supplemental Figure 4: Lactoseries Biosynthesis



**Legend: Fold**



**Supplemental Figure 5: Neolactoseries Biosynthesis**